A GEOSPATIAL ASSESSMENT OF MOUNTAIN PINE BEETLE INFESTATIONS AND THEIR EFFECT ON FOREST HEALTH IN OKANOGAN-WENATCHEE NATIONAL FOREST

Marco Allain, California State University, Bakersfield
Andrew Nguyen, California State University, East Bay
Evan Johnson, University of California, Los Angeles
Emily Williams, University of California, Santa Barbara
Stephanie Tsai, Henry M. Gunn High School
Susan Prichard, Ph.D., University of Washington
Travis Freed, United States Forest Service
J.W. Skiles, Ph.D., NASA Ames Research Center
DEVELOP NASA Ames Research Center
M.S. 242-229 Moffett Field, California 94035
MarcoAllain006@hotmail.com
Joseph.skiles@nasa.gov

ABSTRACT

Fire-suppression over the past century has led to increased forest density and fuel accumulation. Increased stand densities and warm dry summers in the past few decades have predisposed dry, high elevation forest types to mountain pine beetle (MPB) outbreaks. MPB outbreaks occur in three successive stages— the green (initial attack), red (visible attack), and gray (dead) stages. With the use of geospatial technology, these outbreaks can be better mapped and assessed to evaluate forest health. Field work on seventeen randomly selected sites was conducted using the point-centered quarter method. The stratified random sampling technique ensured that the sampled trees were representative of all classifications present. Additional measurements taken were soil nutrient concentrations (sodium [Na^+], nitrate [NO_3^-], and potassium [K^+]), soil pH, and tree temperatures. Finally, satellite imagery was used to define infestation levels and geophysical parameters—such as land cover, vegetation classification, and vegetation stress. ASTER images were used with the Ratio Vegetation Index (RVI) to explore the differences in vegetation, while MODIS images were used to analyze the Disturbance Index (DI). Four other vegetation indices from Landsat TM5 were used to distinguish the green, red and gray phases. Selected imagery from the Hyperion sensor was used to run a minimum distance supervised classification in ENVI, testing the ability of Hyperion imagery to detect the green phase. The National Agricultural Imagery Program (NAIP) archive was used to generate accurate maps of beetle-infested regions.

KEYWORDS: mountain pine beetle, NAIP, NASA Hyperion, Landsat TM, forest fires

INTRODUCTION

Fire suppression and climate change over the last century have predisposed dry forest types to to widespread insect outbreaks (Axelson, 2009). Due to a combination of these factors, bark beetles such as the fir engraver *Scolytus vetralis*, the mountain pine beetle *Dendroctonus ponderosae*, and the western pine beetle *D. brevicomis* have spread rapidly over the last several years (Leatherman, et al., 2007). Such phenomena, specifically warmer climate and drought, have reduced tree defenses to bark beetle attack, leading to increased mortality (Moore, et al., 1993). In addition to natural causes, anthropogenic activities such as fire suppression have contributed to increasingly widespread infestation (Jenkins, et al., 2008). Under normal circumstances, fire acts as a natural control by clearing swaths of forests and ground litter. This slows the growth of stocks and limits competition for water and other necessary resources. However, fire suppression has prevented the natural thinning of the forest. Forests have therefore grown denser with many more water-stressed trees, increasing vulnerability of the forest to bark beetle attacks (Dordel, et al., 2006).

Ground surveys, remote sensing techniques, and aerial detection surveys are the primary methods for monitoring bark beetle infestation (Wulder, et al., 2006). Ground surveys are costly and time consuming, and remote sensing methods have proved to be economical tools for detecting bark beetle damage.

Remote sensing techniques are most effective when bark beetles manifest in homogeneous pockets of mortality. However, outbreaks are rarely homogeneous based on the age of the stand and varying tree species (Miller, et al., 2003). This impairs the accuracy of remote sensing classification models. As a result, it is difficult to understand the magnitude of the problem by exclusively examining satellite imagery. It is therefore necessary that new methodology be created to better understand this problem.

The main objective of this study was to evaluate a widespread and ongoing outbreak in the Okanogan-Wenatchee NF in northern Washington State. The 80,000 ha Tripod fire initiated the spread of the bark beetle infestation in the Okanogan-Wenatchee National Forest in northern Washington State. Bark beetles have a widespread impact, affecting 1.73 of the 22 million acres of forest land in Washington experiencing tree mortality, an increase from previous years (Johnson, et al., 2010). With field work, remote sensing image analysis and an understanding of the phase of infestation, this study identifies specific present and future regions of advanced stress and decline. These findings will aid in the understanding of extensive outbreaks. Goals also include determining differences between mortality and non-mortality sites when analyzing various measures of forest health (Perez and Dragicevic 2009; Sampedro, et al., 2009). Geophysical parameters include vegetation classification, vegetation stress using hyperspectral data, as well as soil and temperature measurements. It has been hypothesized that bark beetle infestation affects tree temperature since it alters the tree's color and therefore its spectral profile. Temperature measurements were taken to test this theory. Vegetation indices used include the Ratio Vegetation Index (RVI) from the ASTER sensor on the NASA Terra Satellite and the Enhanced Wetness Difference Index from Landsat Thematic Mapper 5 (TM5). In addition, Landsat TM5 was used to calculate NDMI (Normalized Difference Moisture Index), NDVI (Normalized Difference Vegetation Index), and DI (Disturbance Index) (Table 1) (Hsu and Johnson, 2008). The MODIS Aqua and Terra sensors were also used to calculate a disturbance index. Image data from the Hyperion satellite will be used in an attempt to identify trees in the first stage of attack.

Bark Beetle Bionomics

Figure 1. Trees produce sap as a defense mechanism when bark beetles borough into the tree, creating pitch tubes.

Mountain Pine beetles attack trees that showcase two favorable characteristics; nutrient content and trunk diameter thickness (Niemann and Visintini, 2005). These factors are thought to attract beetles which then bore into trees and deposit their larvae. Bark beetles are most successful when attacking trees that have been weakened by disease, drought, smog, previous infestations or physical damage. These attacks further weaken the trees, leading to stem deformities, loss of growth, and premature mortality (Moore, et al., 1993).

The mountain pine beetle *(Dendroctonus ponderosae)*, targets ponderosa and lodgepole pines (Leatherman, et al., 2007). The female adult beetle frequents trees with large diameters during late summer (Garrison-Johnston, et al., 2003). In a mass outbreak, beetles may attack smaller diameter trees. The first wave of beetles emits pheromones, drawing more beetles to infested trees, further amplifying infestation (Parker, et al., 2006). Beetles are also attracted to ethanol produced by beetle larvae in the dead, woody tissues.

Figure 2. A red phase tree.

Healthy trees secrete resin, or latex, which contains insecticidal and fungicidal compounds. Such compounds defend the tree against beetle infestations, immobilizing and suffocating the beetles. However, a heavy infestation can overwhelm these defenses, especially in weakened trees, resulting in sawdust-like shavings around the entrance holes (Figure 1, Leatherman, et al., 2007).

Figure 3. A mix of green, red, and gray phase trees.

Tree infestation is a three-stage process (Figure 3). Green attack, the first stage, shows no color change and is therefore difficult to detect with remote sensing. During this stage, the beetles begin to borough through the phloem, interrupting nutrient flow. It takes roughly one year to transition to the second stage, red attack, which can be detected by satellite sensors (Figure 2). The beetle larvae begin to feed on the tree's phloem, starving the tree of nutrients and water, and changing the crown from green to red (Niemann and Visintini, 2005). Gray attack is the final stage in which the tree is dead and has lost all foliage. (Wulder, et al., 2006).

Some natural controls of bark beetle infestations are woodpeckers, which feed on adults and larvae, and extremely cold temperatures (-34C). There are, however, various human-induced controls, including peeling the bark from trees in the green phase to dehydrate the larvae or burning and scorching the logs. Harvesting and thinning suitable host trees are other management options. Chemical control options, however, are very limited since there are no labeled pesticides for use on the beetles (Leatherman, et al., 2007).

Study Site

The Okanogan-Wenatchee National Forest is located south of the Canadian border and east of Cascades National Park in central Washington State (Figure 4). Field sites were located within a 4 km radius of 48.09 latitude and -120.19 longitude. Vegetation within the forest is variable, with small shrubs and grasslands covering the lower elevations. Mid-elevation vegetation primarily consists of ponderosa pine (*Pinus ponderosa*) while lodgepole pine (*P. contorta*), Douglas fir (*Pseudotsuga menziesii*), and subalpine fir (*Abies lasiocarpa*) can readily be found at higher elevations above 1,800 meters.

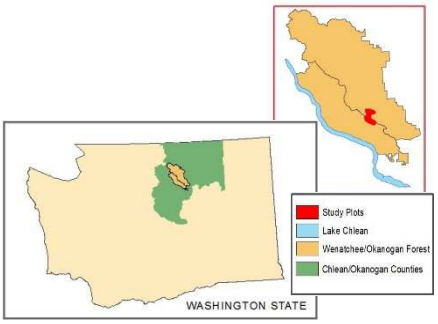

Figure 4. Our study site was located in NE Washington State, directly above Lake Chelan.

The climate is characterized by moderate temperatures during the summer and occasional sub-zero temperatures during the winter months. Recent major droughts occurred in 2001 and 2005. Mean annual precipitation ranges from 30 to 230 centimeters (USDA, 2008). In recent years, the region has experienced severe wildfires. The Deer Point Fire of August 2002 burned stands on the south western edge of our study region. The Tripod Fire burned in excess of 70,820 hectares of the Okanogan wilderness, ranking as one of the largest fires in Washington State over the past 50 years. Fire suppression techniques that began in 1900 have significantly jeopardized the health of the forest by encouraging stock density and increasing competition for resources amongst trees (Iglesias, et al., 1997).

METHODOLOGY

Field Methods

The field study was conducted in June of 2010 to classify forest stands in various stages of attack. This classification creates a base to accurately determine percent infestation, providing a basis of comparison with satellite data. Seventeen primary sampling units (PSU) were measured, each within one of the following categories—severe infestation (red-attack or gray-attack), moderate infestation, and no infestation. Sampling sites were randomly generated, located in polygons derived from areas known to be mountain pine beetle territory in 2009 aerial surveys (Washington State, 2010). Such imagery is useful for narrowing down regions of beetle infestation, providing a preliminary basis for site selection. Selected sites were at least 90 meters and no farther than 500 meters from established roads.

The center of each PSU was located using a real-time differential correction on a Trimble GPS unit. Each coordinate was checked using a Garmin ETrex Vista Hcs handheld GPS. The PSU are 60x60 meters, each consisting of 12 subplots spread across a grid (Cottam, 1953). Subplots consist of three columns spread an equidistant 15 meters apart, with four rows spread at various distances; 10 meters from the northern edge to the first row, 12.5 meters to the second row, 15 meters to the third, 12.5 meters to the fourth, and 10 meters to the southern edge (Figure 4). A laser range finder was utilized to measure the distance from subplot center to the sampled tree. The point-center quarter method (Mitchell, 2007) defined each subplot, in which the four geographical bearings (north, east, south and west) tagged which trees to sample (Figure 5). Measurements taken at each tree included diameter at base height (DBH), distance from sub-plot center, tree species, percent red attack, percent gray attack, presence of pitch tubes, and notable tree discrepancies. This dataset chronicles tree density, species composition, and percent infestation. Further measurements were noted at each plot for percent groundcover, percent understory coverage, and percent over-story coverage. Tree-trunk temperatures were also measured, using a Raytek Raynger ST temperature gun, with measurements taken on the north-facing side of trees. In addition, soil samples were extracted and measured for major nutrient concentrations (K^+, NO_3^- and Na^+) and pH levels at each PSU center point (Moore, et al., 1993). These measurements were made to explore relationships between soil chemical composition and MPB attack behavior.

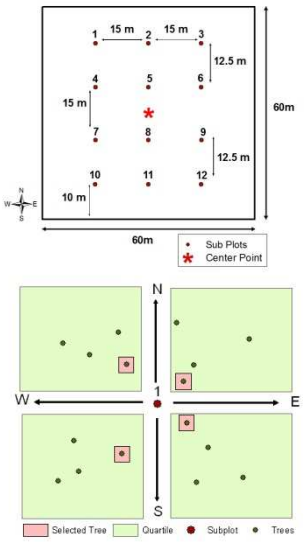

Figure 5. The point-centered method was used to sample each unit.

Unpaired student t-tests were used to determine the effects of soil nutrients (K^+, NO_3^- and Na^+), tree temperature, tree diameter-base-height (DBH) and percent canopy cover on tree mortality (Morehouse, et al., 2008). Percent canopy cover is determined by over-story crown coverage within a five meter radius of each center-plot. Mortality was defined as a unit composed of more than 50% red and gray phases, while non-mortality was defined as more than 50% healthy and green (Perez and Dragicevic, 2009). A p-value of 0.05 or less was used.

Two statistical tests were run to compare mortality with the various indices and contrasting adjacent years' indices. A significance level of 10% was used. An ANOVA test was run on the data from 2002 to 2009 (Table 3). The purpose is to find a correlation between percent mortality and the various indices, so that a model predicting future mortality may be created. The ANOVA compared units were separated into four categories: 0-25% gray, 25-50% gray, 50-75% gray and 75-100% gray. Unpaired student t-tests were run on significant years to observe the differences. The second set of statistical tests compared adjacent years' indices to see if there was an increase or decrease in value from year to year. We used 2-sample t-tests to compare the index values from each yearly pair.

Satellite Image Processing

A combination of MODIS, ASTER, and Landsat satellite imagery were used to detect and quantify percent infestations in the Okanogan-Wenatchee National Forest from 2002 to 2009. Several indices were used, including NDMI, NDVI, DI, EWDI, RVI (Table 1). Comparisons of indices were made to demonstrate the detection strength of each satellite instrument and detect potential future infestation and mortality.

Using Landsat to Create DI, EWDI, NDVI and NDMI Values. For the purpose of this study, 10 Landsat TM5 images were downloaded from the USGS GLOVIS server (http://glovis.usgs.gov/.) Each image was captured during the summer months of June, July, August, or September from 2002 through 2009. All downloaded images were radiometrically corrected in ERDAS Imagine 9.3 and then turned into reflectance values (Wulder, et al., 2006; Chander and Markham., 2003). In total, four spectral indices were calculated; NDVI, NDMI, EWDI, and DI.

The NDVI and NDMI indices were used to detect vegetation and moisture changes in year to year comparisons (Table 1, Eq. 1,2). For the purpose of this study, the vegetation indices were used to detect patches of dead vegetation that correlate with regions of extensive bark beetle infestation. As mountain pine beetle infested stands enter the red phase, NDMI values decrease (Wulder, et al., 2006). The NDMI and the NDVI were calculated in ERDAS Imagine 9.3. Each index was based upon the original reflectance image of each year. NDVI and NDMI indices were then extracted in ArcGIS 9.3 to calculate average pixel values. Coordinate points from the original seventeen field sites were layered atop each vegetation index from each given year, and 2x2 pixel values were averaged.

The tasseled cap (TC) procedure was used to create a vegetation index that measures three vegetation dimensions—brightness, greenness and wetness (Crist and Krauth, 1986). The same procedure was used to create the EWDI, which isolates the wetness layer in two progressive tasseled cap images, differentiating each wetness

layer to detect water stress (Table 1, Equation 3; Skakun, et al., 2003; Han, et al., 2007). In the equation, the variables TC3(2008) and TC3(2009) are the tasseled cap wetness layers from two consecutive years.

Each EWDI was computed in ERDAS Imagine 9.3 for each consecutive year. For instance, the first EWDI differenced August 2002 and July 2003 (Wulder, et al., 2006). The EWDIs were uploaded into ArcGIS 9.3, and a pixel area of 2x2 was used for each sampling site. Pixel reflectance values were obtained and averaged for the seventeen field units.

Further, a disturbance index was calculated based upon tasseled cap images from a single date. The purpose of the disturbance index is to measure vegetation degradation that results from any number of natural or human-induced causes such as forest fires or forest insectic infestations (Hais, et al., 2009). The disturbance index exemplifies the contrast between healthy forest stands and bare ground. Disturbance index images were generated for each year between 2002 and 2009 based upon the original reflectance images—brightness, greenness and wetness (Table 1, Equation 4).

Table 1: Satellite indices used to map stress in Wenatchee and Okanogan Forests

Satellite Indices

Abbreviation	Name	Index	Satellite / Sensor	Description	Reference	#
NDVI	Normalized Difference Vegetation Index	$NDVI = \frac{(NIR - RED)}{(NIR + RED)}$	Landsat	vegetation stress	Rouse *et al*., 1974	1
NDMI	Normalized Difference Moisture Index	$NDMI = \frac{NIR - SWIR}{NIR + SWIR}$	Landsat	Vegetation & water stresses	Jin and Sader, 2005	2
EWDI	Enhanced Wetness Difference Index	EWDI=TC3(2008)-TC3(2009)	Landsat	water stress	Skakun et al., 2003	3
Landsat DI	Landsat Disturbance Index	*DI = Brightness* - (*Greenness* + *Wetness*)	Landsat	tasseled cap based disturbance	Healey *et al*., 2005	4
RVI	Ratio Vegetation Index	$RVI = \frac{NIR}{Red}$	Terra/ ASTER	vegetation stress	Elvidge et al., 1995	5
MODIS DI	Disturbance Index	$DI_{LST/EVI} = \frac{LST_{\max} / EVI_{\max}}{LST_{\bar{x}\max} / EVI_{\bar{x}\max}}$	Terra& Aqua/ MODIS	vegetation & temperature stresses	Mildrexler et al., 2007	6

Using ASTER to Model Beetle Spread. ASTER (Advanced Spaceborne Thermal Emission and Reflection Radiometer) is an imaging instrument supported by Terra, a satellite launched as part of NASA's Earth Observing System (EOS). When vegetation undergoes moisture stress, it reflects low levels of near infrared radiation (NIR) but more red electromagnetic radiation. This results in a decreased RVI with escalated stress (Fettig, et al, 2007). As bark beetles target stressed trees, ASTER's ability to detect stress facilitates validation of infestation. ASTER images were downloaded from the online Warehouse Inventory Search Tool (WIST) website (https://wist.echo.nasa.gov/~wist/api/imswelcome/). The images are dated October 2000, July 2003, August 2005, and July 2008. The limited availability of images prevented a thorough sequential analysis. Vegetation stress was calculated between the four years using the Ratio Vegetation Index (RVI) (Table 1, Equation 5) (Elvidge *et al*., 1995). The four ASTER images were georectified using a geometrically-accurate aerial image and several ground control points as a base. The ASTER images were used to create raster files, which contain the RVI values.

Seventeen polygon shapefiles, each corresponding to a field site, were overlaid on top of the ASTER images. Each polygon occupied a 60x60 meter area, covering a total of sixteen ASTER pixels.

Using MODIS to Create Disturbance Index Archives. MODIS data were used to create the Disturbance Index (DI). When the Land Surface Temperature (LST) and Enhanced Vegetation Index (EVI) contribute anomalies, the

MODIS DI is effective at identifying disturbance. Further, the index better represents the normal ecological condition with the addition of more and more annual mean-maximum values in the denominator (Mildrexler, et al., 2007).

MODIS data were obtained from the Oak Ridge National Laboratory Distributed Active Archive Center (ORNL DAAC) website (http://daac.ornl.gov/MODIS/). Data from years 2002 through 2009 were compiled from the DAAC server. Seventeen data sets were requested—one set for each PSU. As delineated by Mildrexler *et al.* (2007), LST and EVI were used to create the MODIS Disturbance Index (Table 1, Equation 6). LST data is gathered from the Aqua/MODIS eight-day composite daytime sensor. EVI data is gathered from the Terra/MODIS 16-day composite sensor.

Landsat Classification. In order to assess the ability of Landsat to detect red-phase trees, an ISODATA unsupervised classification was conducted. Vegetation classes were narrowed to four categories – healthy forest, red-phase forest, bare ground and shrubbery, and ice.

Satellite Image Processing—Hyperspectral Detection of the Green Phase. Research has shown that Landsat TM5 is successful in detecting the red and gray phases of bark beetle attack, but not the green phase (White et al., 2007). Our study is aimed at determining if Hyperion is indeed able to differentiate between the green phase and healthy trees.

Preprocessed Landsat images from 2002 and 2003 were used to train Hyperion data. Previous studies have shown that there is a twelve month time period to reach 90% red phase from an initial 100% green phase (Wulder, 2006). Using this information, a supervised minimum distance classification was run on the Landsat images, searching for green and red trees. This classification used predefined "regions of interest," or ROIs, specific to each year, containing purely green pixels in 2002 and red pixels in 2003. The 2002 and 2003 Landsat classifications were then overlaid to find pixels classified in each year. Forty-six pixels were found and defined as green phase ROIs. The spectra of both green phase and non-green phase pixels were graphed and compared to determine what bands fluctuate with the green phase. Two supervised spectral angle mapper classifications were run on the Hyperion image, using 20 merged green phase ROIs per classification. We compared the two classified images, looking for a correlation between classified pixels. An accuracy of 50% or higher indicates success (Subramanian, et al., 1997).

Using NAIP Imagery to Quantify the Infestation

The National Agriculture Imagery Program (NAIP) provides detailed, high resolution images acquired by aircraft of the entire United States. Digital NAIP imagery is useful for visualizing and quantifying the extent of the mountain pine beetle infestation as a result of its 1-m resolution. Each image contains spatially detailed ground information, allowing differentiation between red and green crowns. Red pixels have markedly different values in the multispectral NAIP imagery than do green pixels. A simple algorithm was used to identify red crown pixels based on visual inspection of the imagery (Equation 7).

$$\left\{\left[\left(\frac{\mathrm{Re}\,d}{Green}\right) < (Threshhold_{\mathrm{Re}\,d\,/\,Green})\right] * [Blue < Threshhold_{Blue}]\right\} * [255] \qquad \text{(Equation 7)}$$

ERDAS Imagine was used to create a model which runs a raster NAIP image from a particular year through this algorithm. It is important to recognize that every NAIP image will have different threshold values dependent on the quality and time of day of the image. The algorithm sets to zero all pixels that do not meet the specified characteristics as defined by the unique threshold value. Such manipulation permits the creation of detailed maps that chronicle the amount of trees with red crowns in a given area. With one meter resolution, acreage of infestation can be calculated based upon the number of red pixels in a given area.

The binomial probability theory equation was utilized to determine the number of points that should be selected for the accuracy assessment (Jensen, 2007). The equation is defined below:

$$N = \frac{Z^2(p)(q)}{E^2}$$

This was computed where N is the sample size, $Z = 2$ from the standard deviate of 1.96 for the 95% two-sided confidence level, p is the expected accuracy for the entire map, $q = 100 - p$, and E is the allowable error (Jensen, 2007). The number of random sample locations was computed as:

$$75 = \frac{2^2(75)(25)}{10^2}$$

This amounted to 75 points with an expected accuracy of 75% and a 10% allowable error.

RESULTS

Field Measurements

Table 2: Statistics run on field measurements (T-Test).

Site Class	% canopy cover	Tree Temperature	[NO3-]	[K+]	[Na+]
> 50% red/gray	54.11 ± 77.14	20.0 ± 3.40*	77.13 ± 46.80	385.7 ± 220.4	271.67 ±214.24
< 50% red/gray	56.18 ± 23.71	16.3 ± 2.31	67.00 ± 27.91	456 ± 214	292.22 ±248.64

Confidence intervals at the 10% level; asterisks denote statistical significance.

At the 5% level, lodgepole pine trees were warmer than other tree species during midday ($p < 0.001$), yet there was no significant difference between the morning ($p=0.795$) and afternoon ($p=0.9249$). Gray trees had the same significantly higher temperatures compared to all live trees at midday ($p=2.077 \times 10^{-8}$). Nutrient concentrations for NO_3^- ($p=0.62$), K^+ ($p=0.524$) and Na^+ ($p=0.867$) as well as percent canopy cover ($p=0.7975$) had no significant correlation with tree mortality (Table 2). In summation, grey trees exhibited higher temperatures than healthy trees.

Indices. Within the study region, the four indices—NDMI, NDVI, EWDI and DI—were statistically different in year-to-year comparisons (Appendix 1). The years with the greatest differences were 2002 to 2003, 2004 to 2005, and 2006 to 2007.

Two years displayed the highest moisture and vegetation levels—2002 and 2006. These years had significantly more moisture (NDMI), or less moisture stress (EWDI), than 2003 and 2007, respectively (Figure 6). Also, 2002 and 2006 had greater levels of vegetation and a lower disturbance than their respective consecutive years. This data correlates to the drought in 2003 (-2.75 and below) (State of the Climate, 2009).

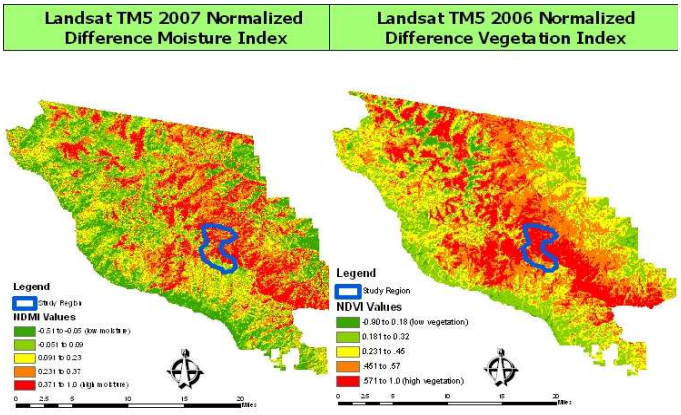

Figure 6. NDVI and NDMI were created using Landsat.

However, 2004 had significantly lower levels of vegetation yet lower moisture stress than 2003. It also showed lower Landsat disturbance yet higher MODIS disturbance levels than 2003. Since 2002, the MODIS sensor has detected increasing disturbance levels at unhealthy sites, especially between 2006 and 2009 (Figure 7).

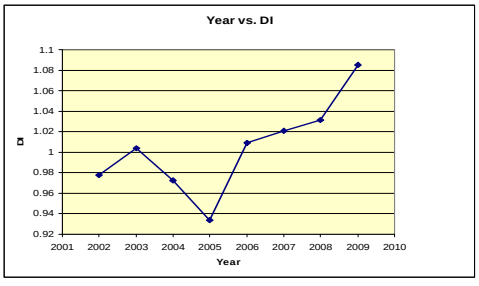

Figure 7. DI Average for years 2002 to 2009 inclusive.

RVI (ratio vegetation index) derived from the ASTER imagery showed no significant differences between any of the years.

Low mortality sites (those with less than 25% gray trees) had significantly more vegetation (from NDVI) than the higher mortality sites for years 2003, 2007, 2008 and 2009. High mortality sites showed lower Landsat disturbance levels, yet higher MODIS disturbance levels, than low mortality sites, as demonstrated by the years 2006, 2008 and 2009. The

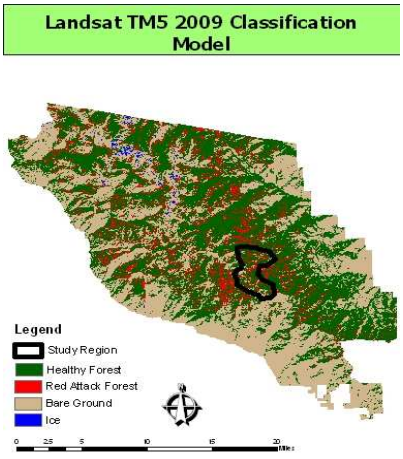

Figure 8. A classification was run on the Landsat 2009 image.

EWDI indices also demonstrated less moisture stress for high mortality sites, yet the NDMI held significance for high mortality sites having a low moisture content (demonstrated by years 2007, 2008 and 2009).

Landsat Classification

The classification achieved an overall classification score of 80%. However, the classification was only 39.53% accurate in detecting red-phase forest (Figure 8). Accuracy was calculated using the ERDAS Imagine accuracy assessment tool.

Table 3: Indices Comparison Between Mortality Categories (ANOVA tests' values)

* = statistical significance at the 10% level

	MODIS DI (disturbance index)	Landsat DI (disturbance index)	NDVI (vegetation level)	NDMI (moisture level)	EWDI (moisture stress)
2002	p=0.7100	p=0.9887	p=0.4125	p=0.7424	p=0.7414
2003	p=0.1858	p=0.2830	p=0.0871*	p=0.1657	p=0.4592
2004	p=0.3579	p=0.8470	p=0.1271	p=0.3132	p=0.4597
2005	p=0.1707	p=0.3819	p=0.1201	p=0.2255	p=0.9749
2006	p=0.0854*	p=0.3902	p=0.2546	p=0.7163	p=0.2695
2007	p=0.5531	p=0.8265	p=0.0011*	p=0.0798*	p=0.0170*
2008	p=0.8724	p=0.0410*	p=0.0066*	p=0.0282*	p=0.4621
2009	p=0.9598	p=0.0454*	p=$7.04e^{-5}$*	p=0.0003*	N/A

Detection of the Green Phase

Hyperion satellite imagery was able to classify the green phase, with a kappa coefficient of 0.1163, or 11.63%. As the kappa coefficient disregards chance agreement, this was a significant finding. This finding was supported by comparing the spectra of the green phase and healthy trees.

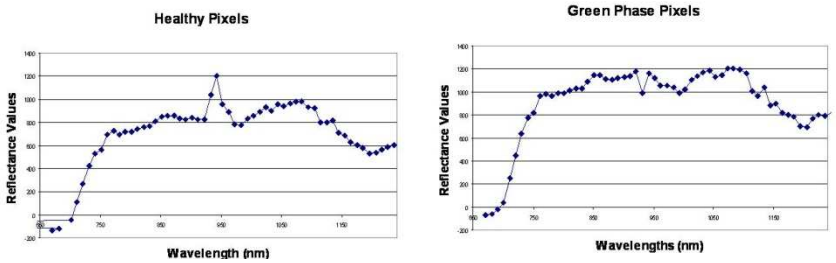

Figure 9. A comparison between the spectra of green phase pixels and healthy pixels.

The green phase emitted at higher reflectance values (by approximately 200 µW/(cm^2*sr*nm)) between wavelengths of 671nm to 1336 nm (band numbers 32 through 119) (Figure 9). In Cheng, et al., 2010, it was found that the green phase is characterized by its moisture content between wavelengths of 1318 nm and 1322 nm. Our findings therefore indicate that green phase trees emit higher reflectance values in the red portion of the spectrum, due to decreased chlorophyll content, and in the infrared portion of the spectrum, due to decreased water content.

Hyperion is an efficient tool at detecting the green phase. The accuracy level can be increased by using ground data as training data and NAIP imagery to run the accuracy assessment against.

NAIP Red Phase Algorithm

NAIP imagery was successful in detecting the extent of the red phase. Accuracy was measured in ArcGIS by random selection of points located within red tree clusters.

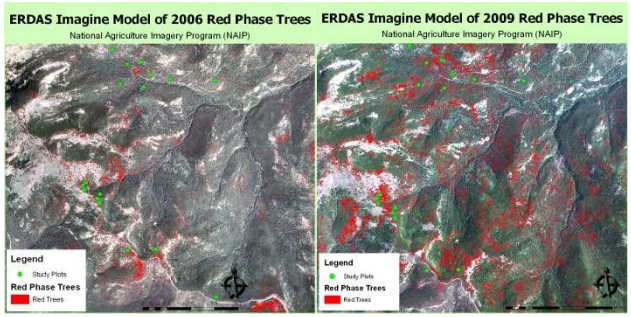

Figure 10. Depiction of red phase in NAIP imagery.

This accuracy assessment demonstrates that the algorithm and classification is 96% accurate. The total acreage of the study region shown above is 38,481,540 square meters (Figure 10). In 2006, red phase trees covered 146,188 square meters. By 2009, this number rose to 4, 151,500 square meters.

DISCUSSION

Classification schemes are an effective way to categorize large areas without detailed imagery. The Landsat classification had an overall accuracy of 80%, yet was only 39.53% accurate at detecting the red phase. This is due to the 30x30 meter resolution of the imagery and non-homogeneity of the sites. Non-homogenous sites were often inaccurately classified. Inaccurate classifications were the result of border pixels and mixed pixels. If a pixel is 60% green phase and 40% red phase, the classification scheme will display it as being 100% green phase. Pixels that occur along the border of different classes are also frequently misidentified. However, an algorithm was created to detect the red phase in NAIP imagery. This may be used in tandem with hyperspectral imagery, such as Hyperion, to improve the accuracy of the detection of beetle infestation.

The Hyperion classification of the green phase also had a low accuracy level, with a kappa coefficient of 0.1163. However, Hyperion was able to detect that the green phase in the reflectance in the red and infrared regions of the electromagnetic spectrum. The higher reflectance in the red region (620 nm to 780 nm) may be due to the reduced chlorophyll content of infested trees (Ahern, 1988). Trees with lower chlorophyll content tend to reflect rather than absorb red wavelengths. Therefore, infested trees will have a higher red reflectance level than healthy trees. The higher infrared reflectance is caused by decreased water flow to the crown, due to the burrowing of the bark beetles (Hicke and Jenkins, 2008). Hyperion's ability to detect the spectral differences between green and other phase trees indicates that Hyperion may be used to detect the green phase, although a further accuracy analysis should be pursued. It may also be a strong predictor of the red phase, with its hyperspectral capabilities.

The NDMI and EWDI spectral indices were fairly accurate in detecting droughts and fires, as checked by NOAA's archive of droughts and wildfires. However, several years (such as 2006 and 2008) were not drought years yet appeared dry in the NDMI. The EWDI indicated increasing moisture stress over several years that, in fact, were undergoing less severe droughts. The two disturbance indices strongly correlated with moisture stress (EWDI), and prove to be very reliable. The NDVI also had a strong correlation with the NDMI, indicating that moisture levels are sound indicators of vegetation levels, and vice versa.

The field measurements and NAIP photos were useful for training satellite data and understanding the extent of mountain pine beetle infestation. Tree temperatures taken in the field may be used as a secondary indicator of tree health and beetle infestation. Gray phase trees have little to no water, thus increasing the tree's temperature. On average, lodgepole pine trees had the same elevated temperatures as gray phase trees. These findings will allow for the improved detection and, therefore, management, of beetle infestations. A combination of satellite imagery classifications, spectral indices, and field data can better predict high risk areas.

The aforementioned methods can be applied in infestation mitigation practices. This study is strong evidence that spectral indices can be used to detect areas of infestation. Also, the NAIP algorithm which was derived can be modified and used to display red phase trees in any NAIP image. With this new algorithm, acreage of infested areas can be quickly determined with 96% accuracy. This information can help the forest service predict future sites of infestation. Future studies should focus on using Hyperion data to more accurately classify the incipient green phase. The green phase can be accurately detected with extensive field work and high resolution NAIP images, which can both be used to train an accurate supervised classification.

CONCLUSION

Remote sensing is a valuable tool in tracking bark beetle infestation. However, the size of infested areas tends to be small relative to satellite resolution. Thus, high spatial resolution imagery is optimal. Resolution of the aforementioned satellites was sufficient for the purposes of this initial study, but more detailed imagery would yield better results for the spectral indices. The five multispectral indices proved to be accurate at detecting infestation. This is because moisture content, vegetation levels, and ecosystem disturbance are all related to infestation. Multiple measurements per sampling site would likely yield more significant results. Temperature, however, does correlate to the level of beetle infestation.

Hyperion can differentiate between the red and infrared portions of the spectra of green phase and healthy trees. Hyperion, therefore, shows promise at detecting the green phase, although further research should be done to increase the accuracy of Hyperion's classification of the green phase. This study is intended to map the distribution and extent of bark beetle infestation in Okanogan-Wenatchee National Forest. Through the usage of field work, spectral indices, and NAIP imagery, bark beetle infestation can be detected so that any necessary mitigation steps can be taken.

ACKNOWLEDGEMENTS

We sincerely thank Dr. Jennifer Dungan, Lee Johnson, Brad Lobitz, and Dr. Charles Williams for their assistance with GIS and remote sensing.

Appendix 1

Appendix 1: Year to Year Comparisons for Five Indices

* = statistical significance at the 10% level

	MODIS DI (disturbance index)	Landsat DI (disturbance index)	NDVI (vegetation level)	NDMI (moisture level)	EWDI (moisture stress)
2002-2003	Increase p=0.0165*	Increase p=3.3e^{-5}*	Decrease p=1.603e^{-8}*	Decrease p=1.185e^{-9}*	Increase p=3.083e^{-9}*
2003-2004	Decrease p=0.0130*	Decrease p=1.039e^{-5}*	Decrease p=0.3418	Decrease p=0.1598	Decrease p=1.639e^{-11}*
2004-2005	Decrease p=0.0213*	Increase p=6.504e^{-4}*	Increase p=4.198e^{-7}*	Increase p=0.2197	Increase p=0.00*
2005-2006	Increase p=3.439e^{-4}*	Increase p=0.4129	Decrease p=0.2331	Increase p=1.0496e^{-7}*	Increase p=1.784e^{-4}*
2006-2007	Increase p=0.2523	Increase p=0.0389*	Decrease p=0.0222*	Decrease p=0.0634*	Increase p=1.771e^{-4}*
2007-2008	Increase p=0.2556	Decrease p=0.0906*	Decrease p=0.4517	Decrease p=0.0163*	Decrease p=0.2122
2008-2009	Increase p=0.0062*	Increase p=0.3190	Decrease p=0.0691*	Increase p=0.0594*	N/A

REFERENCES

Axelson, N.J. (2009). Influence of fire and mountain pine beetle on the dynamics of lodgepole pine stands in British Columbia, Canada. *Forest Ecology and Management*, 257, 1874 – 1882.

Ahern, F.J. (1988). The effects of bark beetle stress on the foliar spectral reflectance of lodgepole pine. *International Journal of Remote Sensing*, 9: 9, 1451 – 1468.

Chander, G.; Markham, B. (2003). Revised landsat-5 TM radiometric calibration procedures and post-calibration dynamic ranges. *IEEE Transactions on Geoscience and Remote Sensing*, 41(11): 2674-2677.

Cheng, T.; Rivard, B.; Sanchez-Azofeifa, G.A.; Feng, J.; Calvo-Polanco, M. (2010). Continuous wavelet analysis for the detection of green attack damage due to mountain pine beetle infestation. *Remote Sensing of Environment*, *114*.

Cottam, G. (1953). Some Sampling characteristics of a population of randomly dispersed individuals. *Ecology*, *34*(4), Retrieved from http://www.jstor.org/stable/1931337

Crist, E.P.; Kauth, R.J. 1986. The tasseled cap de-mystified. *Photogrammetric Engineering & Remote Sensing*, 52(1): 81-86.

Dordrel, J.; Feller, C.M; Simmard, S. (2008). Effects of mountain pine beetle (Dendroctonus ponderosae Hopkins) infestations on forest stand structure in the southern Canadian Rocky Mountains. *Ecology and Management*, 255, 3563.

Elvidge, C.D.; Yuan, D.; Weerackoon, R; Lunetta, R. (1995). Relative radiometric normalization of Landsat multispectral scanner (MSS) data using an automatic scattergram-controlled regression. *Photogrammetric Engineering and Remote Sensing.* 61(10):1255-1260.

Fettig, C. 2007. The Effectiveness of Vegetation Management Practices for Prevention and Control of Bark Beetle Infestations in Coniferous Forests of the Western and Southern United States. Forest Ecology and Management 238: 24-53.

Garrison-Johnston, M.; Moore, J.; Cook, S.; Niehoff, G. (2003). Douglas-fir beetle infestations are associated with certain rock and stand types in the inland northwestern united states. *Community and Ecosystem Ecology*, *32*(6).

Hais, M.; Jonasova, M.; Langhammer, J.; Kucera, T. (2009) Comparison of two types of forest disturbance using multitemporal landsat TM/ETM+ imagery and field vegetation data. *Remote Sensing of Environment.* 113: 835-845.

Han, T.; Wulder, M.; White, J.; Coops, N.; Alvarez, M.; Buston, C. (2007). An Efficient protocol to process landsat images for change detection with tasselled cap transformation. *IEEE Geoscience and Remote Sensing Letters*, *4*(1).

Healey, S.; Cohen, W.B.; Zhiqiang, W.; Krankina, O.N. 2005. Comparison of Tasseled Cap-based Landsat data structures for use in forest disturbance detection. *Remote Sensing of Environment.* 97: 301-310.

Hicke, A.J.; Jenkins, C.J. (2008). Mapping lodgepole pine stand structure susceptibility to mountain pine beetle attack across the western United States. *Forest Ecology and Management*, 255, 1536 – 1547.

Hsu, C.; Johnson, L. (2008). Multi-criteria wetlands mapping using an integrated pixel-based and object-based classification approach. *Colorado Department of Transportation*, *CDOT*.

Iglesias, T.; Cala, V.; Gonzalez, J. (1997). Mineralogical and chemical modifications in soils affected by a forest fire in the mediterranean area. *The Science of the Total Environment*, *204*(89-94).

Jenkins, J.N.; Herbertson, E.; Page, W.; Jorgensen, A.C. (2008). Bark beetles, fuels, fires and implications for forest management in the Intermountain West. *Forest Ecology and Management*, 254, 16 – 34.

Jensen, J. 2007. *Remote Sensing of the Environment an Earth Resource Perspective*, edited by D. Kaveney, J. Howard, K. Schiaparelli, and E. Thomas. Upper Saddle River, NJ: Pearson Prentice Hall.

Jin, S., and Sader, S.S. 2005. Comparison of time series tasseled cap wetness and the mormalized difference moisture index in detecting forest disturbances. *Remote Sensing of Environment. 94:* 364-372.

Johnson, M.; Kohler, G.; Omdal, D.; Ramsey-Kroll, A.; Hostetler, B.; Mathison, R.; Nelson, A. (2010). Forest health highlights in washington--2009. *USDA.*

Leatherman, D.; Aguayo, I.; Mehall, T. (2007). Mountain pine beetle. *Insect Series*, *5*(528).

Mildrexler, D.J.; Zhao, M.; Heinsch, F.; Running, S. (2007) A new satellite-based methodology for continental scale disturbance detection, *Ecological Applications*, 17(1): 235-250.

Miller, J.D.; Danzer, S.R.; Watts, J.M.; Stone, S.; Yool, S.R. (2003). Cluster analysis of structural stage classes to map wildland fuels in a madrean ecosystem. *Journal of Environmental Management*, *68*(3).

Mitchell, K. (2007). Quantitative analysis by the point-centered quarter method. *Hobart and Williams Smith Colleges.*

Moore, J.; Mika, P.; Schwandt, J.; Shaw, T. (1993). Nutrition and forest health. *Interior Cedar-Hemlock-White Pine Forests: Ecology and Management.*

Morehouse, K.; Johns, T.; Kaye, J.; Kaye, M. (2008). Carbon and nitrogen cycling immediately following bark beetle outbreaks in Southwestern ponderosa pine forests. *ScienceDirect*, *255*(7).

Niemann, K.; Visintini, F. (2005). Assessment of potential for remote sensing detection of bark beetle-infested areas during green attack: a literature review. *Natural Resources Canada*.

Parker, J.T; Clancy, M.K; Mathiasen, L.R. (2006). Interactions among fire, insects and pathogens in coniferous forests of the interior western United States and Canada. *Agriculture and Forest Entomology*, 8, 167 – 189.

Perez, L.; Dragicevic, S. (2009). Modeling mountain pine beetle infestation with an agent-based approach at two spatial scales. *Environmental Modeling & Software*, 25(2).

Rouse J.W., Haas R.H., Schell J.A. and. Deering D.W, Monitoring vegetation systems in the Great Plains with ERTS, *Proceedings of the Third Earth Resources Technology Satellite-1 Symposium*, NASA, Greenbelt, MD (1974), pp. 301–317.

Sampedro, L.; Moreira, X.; Martins, P.; Zas, R. (2009). Growth and nutritional response of *Pinus pinaster* after a large pine weevil (*Hylobius abietis*) attack. *Trees, 23.*

Skakun, R.S.; Wulder, M.; Franklin, S. (2003). Sensitivity of the thematic mapper enhanced wetness difference index to detect mountain pine beetle red-attack damage. *Remote Sensing of Environment,* 86, 433-443.

State of the Climate drought, annual 2005. (2009). *National Oceananic and Atmospheric Administration.*

Subramanian, S.; Gat, N.; Sheffield, M.; Barhen, J.; Toomarian, N. (1997). Methodology for hyperspectral image classification using novel neural network. *Algorithms for Multispectral and Hyperspectral Imagery III, SPIE, 3071.*

United States Department of Agriculture, Natural Resources Conservation Service. 2008. Soil Survey of Okanogan National Forest Area, Washington. Accessible online at: http://soils.usda.gov/survey/printed_surveys/.

Washington State Department of Natural Resources, . (Photographer). (2010). *Usgs 100k quad: twisp- a148120*. [Web]

White, J.C.; Coops, N.; Hilker, T.; Wulder, M.; Carroll, A. (2007) 'Detecting mountain pine beetle red attack damage with EO-1 Hyperion moisture incides', International Journal of Remote Sensing, 28: 10, 2111—2121.

Wulder, M.A.; White, J.C.; Coops, N.C.; Han, T.; Alvarez, M.F.; Butson, C.R.; Yuan, X. (2006). A Procedure for mapping and monitoring mountain pine beetle red attack forest damage using landsat imagery. *Canadian Forest Service, BC-X-404*.